NREL
NATIONAL RENEWABLE ENERGY LABORATORY

Downscaling Solar Power Output to 4-Seconds for Use in Integration Studies

Preprint

M. Hummon, A. Weekley, K. Searight, and K. Clark

To be presented at the 3rd International Workshop on Integration of Solar Power in Power Systems
London, England
October 21–22, 2013

NREL is a national laboratory of the U.S. Department of Energy
Office of Energy Efficiency & Renewable Energy
Operated by the Alliance for Sustainable Energy, LLC.

This report is available at no cost from the National Renewable Energy Laboratory (NREL) at www.nrel.gov/publications.

Conference Paper
NREL/CP-6A20-60335
October 2013

Contract No. DE-AC36-08GO28308

This report is available at no cost from the National Renewable Energy Laboratory (NREL) at www.nrel.gov/publications.

Available electronically at http://www.osti.gov/bridge

Available for a processing fee to U.S. Department of Energy and its contractors, in paper, from:

U.S. Department of Energy
Office of Scientific and Technical Information
P.O. Box 62
Oak Ridge, TN 37831-0062
phone: 865.576.8401
fax: 865.576.5728
email: mailto:reports@adonis.osti.gov

Available for sale to the public, in paper, from:

U.S. Department of Commerce
National Technical Information Service
5285 Port Royal Road
Springfield, VA 22161
phone: 800.553.6847
fax: 703.605.6900
email: orders@ntis.fedworld.gov
online ordering: http://www.ntis.gov/help/ordermethods.aspx

Cover Photos: (left to right) photo by Pat Corkery, NREL 16416, photo from SunEdison, NREL 17423, photo by Pat Corkery, NREL 16560, photo by Dennis Schroeder, NREL 17613, photo by Dean Armstrong, NREL 17436, photo by Pat Corkery, NREL 17721.

Printed on paper containing at least 50% wastepaper, including 10% post consumer waste.

Downscaling Solar Power Output to 4-Seconds for Use in Integration Studies

Marissa Hummon, Andrew Weekley, Keith Searight, Kara Clark
National Renewable Energy Laboratory
Golden, CO
Author contact: marissa.hummon@nrel.gov

Abstract— **High penetration renewable integration studies require solar power data with high spatial and temporal accuracy to quantify the impact of high frequency solar power ramps on the operation of the system. Our previous work concentrated on downscaling solar power from one hour to one minute by simulation. This method used clearness classifications to categorize temporal and spatial variability, and iterative methods to simulate intra-hour clearness variability. We determined that solar power ramp correlations between sites decrease with distance and the duration of the ramp, starting at around 0.6 for 30-minute ramps between sites that are less than 20 km apart. The sub-hour irradiance algorithm we developed has a noise floor that causes the correlations to approach ~0.005. Below one minute, the majority of the correlations of solar power ramps between sites less than 20 km apart are zero, and thus a new method to simulate intra-minute variability is needed. These intra-minute solar power ramps can be simulated using several methods, three of which we evaluate: a cubic spline fit to the one-minute solar power data; projection of the power spectral density toward the higher frequency domain; and average high frequency power spectral density from measured data. Each of these methods either under- or over-estimates the variability of intra-minute solar power ramps. We show that an optimized weighted linear sum of methods, dependent on the classification of temporal variability of the segment of one-minute solar power data, yields time series and ramp distributions similar to measured high-resolution solar irradiance data.**

Keywords – downscaling solar power; solar power integration; automatic generator control; power spectral density; solar power variability

I. INTRODUCTION

Integration studies of solar power range from capacity expansion to operations and production cost to high-frequency transient stability analysis. The impact analysis framework of each integration study defines the geographic and temporal scope, as well as the resolution of the input data. For instance, production cost operation studies require solar power data with temporal resolution less than 5-minutes in order to accurately calculate operating reserve requirements [1] and 5 to 60 minutes to optimize the unit commitment and economic dispatch models [2,3]. The distance between injection busses in the transmission or distribution network often determines the geographic resolution required for the solar power data. Aggregation of point source solar power data to the injection busses should show a reduction of solar power variability with an increase in area "covered" by the aggregated data [4]. In addition, the solar data set should be coherent across geographic and temporal scales, such that nearby sites have a higher degree of correlation in the change in solar power output (ramp) than sites that are further apart. Likewise, ramps with a shorter duration have a lower correlation between two sites than longer duration ramps [2,5].

The power system balances generation and load on a second-to-second basis via several mechanisms including automatic generator control (AGC). The majority of demand is met by scheduling generation units 24 to 36 hours in advance to come online. However, system operators also schedule "spare" capacity to make up any real time differences between the schedule generation and the actual demand [6]. The rules and procedures for balancing the system by deploying operating capacity, at time scales of less than 5-minutes, are based on a long history of operating the system. High temporal resolution solar data enables researchers to explore new methods of balancing the system [7], as the penetration of variable generation increases. This paper consists of four sections: overview of the four-second algorithm (FSA), analysis of four-second variability, modelling of four-second variability, and comparing the FSA outputs to measured data.

II. FOUR-SECOND ALGORITHM OUTLINE

The FSA was designed on two premises. First, the correlation between changes in solar power output over a time interval of 4-seconds at one site are uncorrelated with simultaneous ramps at any other site in the system. In other words, the cloud properties that cause high frequency changes in solar power are uncorrelated over the region. Indeed, below one minute, the majority of the correlations of solar power ramps between sites less than 20 km apart are zero. Second, the variability of the 4-second solar power ramps is related to the 1-minute solar power ramp variability. Thus, if the 1-minute solar power values are smooth, we expect that the 4-second solar power values are also smooth. Fig. 1 outlines the steps in the FSA. The first step is converting the solar irradiance data to clearness index (measured solar data divided by the clear sky expected solar data), which removes the diurnal shape of the solar data. The second step segments the data into 60-minute periods for analysis and computation. There are four phases for step 2: classify the variability (discussed in Section III), calculate the fast Fourier transform (FFT), model high frequency behavior (discussed in Sections IV

and V), and calculate the inverse FFT (IFFT). Step 3 concatenates the segments of modelled 4-s data, removes discontinuities, and applies the appropriate spatial filter. Step 4 rescales the clearness index data to irradiance data. Weekley et al. (2013) provides a thorough discussion of the downscaling method described in this paper, see Ref. [8]. Other groups have pursued algorithms for downscaling solar power data from satellite images [9], and from numerical weather prediction models [10].

III. High-Frequency Solar Data

To estimate the values of 4-second time interval solar power from 1-minute values of solar power, we used two datasets of ground measured solar global horizontal irradiance (GHI) with a temporal resolution of 1-second. The Oahu dataset consists of 17 irradiance sensors covering an area of 0.25 km^2, which represents approximately a 10 MW photovoltaic power plant [11]. The Golden dataset consists of 4 irradiance sensors in close proximity [1]. A single day of simultaneous global horizontal irradiance from all sensors in the Oahu dataset is shown in Fig. 2a, the average of the sensors is shown in Fig. 2b.

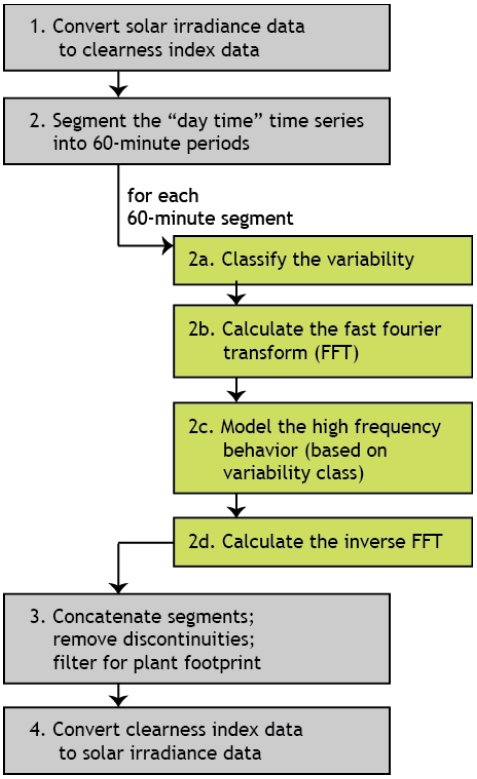

Figure 1. Outline of the four-second algorithm.

As stated earlier, we expect the ramps in the 4-second data to be related to the ramps in the 1-minute data. In order to classify the temporal variability, we calculate the clear sky GHI (GHI_{clear}) for each location/time step and then calculate the clearness index: GHI_{meas}/ GHI_{clear}. Each 60-minute segment per dataset is assigned to one of six classes of clearness index temporal variability (classes are shown in Fig. 3). These classes of temporal variability are described primarily by the standard deviation of the clearness index ramps, from smoothly varying cloud cover (Class I) to cumulus cloud cover (Class V). Further discussion of the clearness index classification can be found in Ref. [2]. We use the temporal classification of the 1-minute data as an input to the algorithm because the high frequency characteristics of the time series are separable by temporal class. For instance, Fig. 4 shows the time series and power spectral density of a segment from the Oahu dataset, classified as Class V.

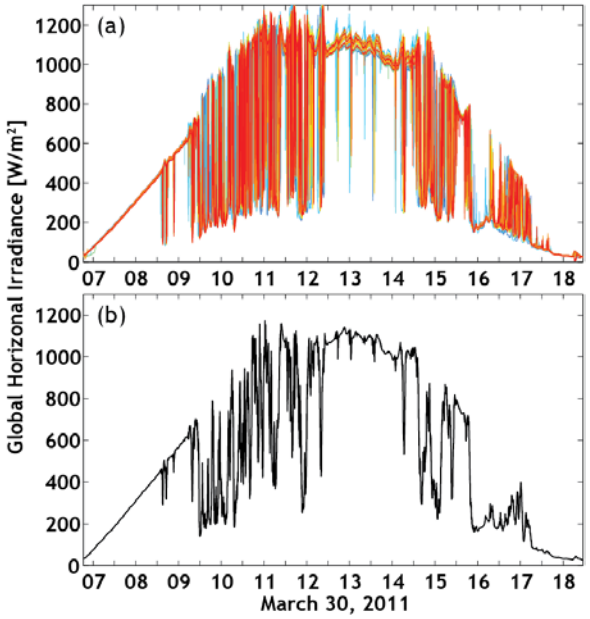

Figure 2. Global horizontal irradiance time series for individual sites (upper) in the Oahu dataset and the average of all 17 sites (lower).

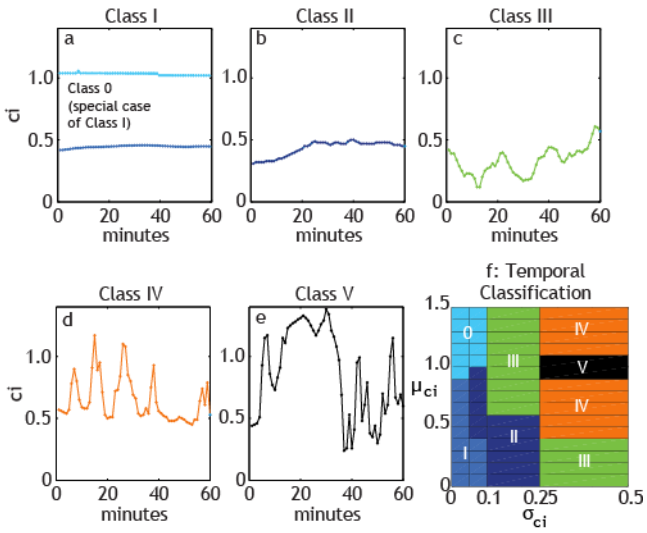

Figure 3. Examples of the five classes of temporal variability are shown in plots (a) through (e). Classes I-III (a-c) are based on the width of the distribution of ramps. Classes IV-V (d,e) are characterized by a rapid change between two or more different cloud cover densities (e.g., clear sky with small, dense clouds moving at a high altitude). Panel (f) shows how the temporal classes are defined in terms of the mean (μ_{ci}) and standard deviation (σ_{ci}) of the clearness index for 60 consecutive minutes.

[1] The sensors located at the National Renewable Energy Laboratory are part of the Measurement and Instrumentation Data Center (MIDC): http://www.nrel.gov/midc/

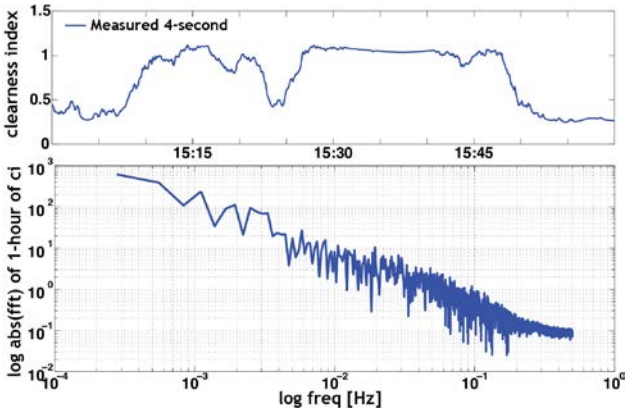

Figure 4. Time series and power spectral density of one hour (Class V) of clearness index with 4-second resolution.

The power spectral density demonstrates the magnitude of each frequency in the time series [12]. Fig. 5 demonstrates the average power spectral density (PSD) of the 1-second data for each temporal variability class, calculated by analyzing all of the high frequency measured data in the Oahu dataset over a year. The classes with the least variability have the lowest amplitude of power spectral density across all frequencies. The average PSD is one of four downscaling methods that are linearly summed with class-specific optimal weighting to estimate the high-frequency behavior of the solar PSD (described in Section V).

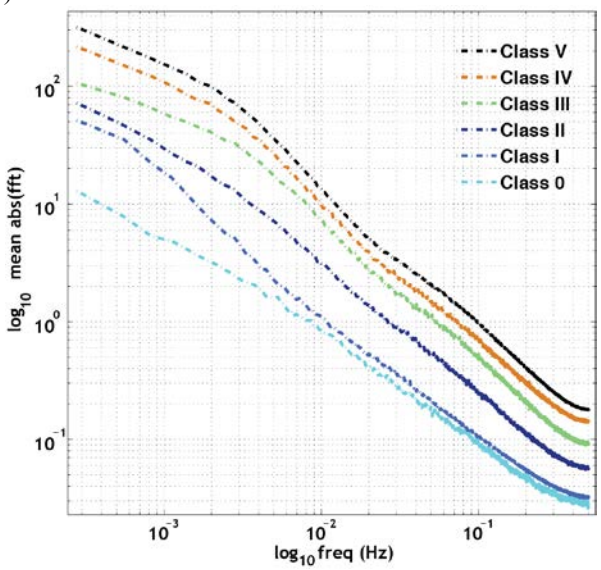

Figure 5. Average spectral amplitude for Oahu dataset, shown as a function of temporal variability class.

IV. Modelling Four-Second Variability

The average PSDs underestimate the variability observed in measured 4-second data. We test this by comparing the ramps of the modelled data resulting from the IFFT to the ramps of the measured 4-second. The average plots of the solar PSD appear to be linear in log-log space, which is suggestive of a power law. Regions of differing slope suggest that the physical processes that cause variability are not continuous across all times scales. For instance, the physics of cloud formation, movement, and dissipation drive variability on time scales between 1-minute and 20-minutes. However, variability below 1-minute might be driven by the internal movement of clouds.

Fig. 6 shows two additional methods for estimating the PSD in the high frequency region. Starting with the PSD of the 1-minute data (the input to the four-second algorithm), we use a linear fit to either all of the frequencies in the 1-minute PSD (black line) or the frequencies between 0.004167 and 0.00833 (2 to 4 minutes, pink line) which is the higher half of the 1-minute PSD frequencies. The fit over all frequencies is representative of the general trend during the hour, while the fit over the higher frequency region, which tends to have a shallower slope, suggests that the variability of the data on time scales near 2-minutes is larger than the higher frequency data.

We compare the distribution of 4-second ramps using the linear fits in Fig. 6, as well as a cubic spline fit to the 1-minute data. The linear fit over a subset of frequencies generally overestimated the magnitude of the 4-s ramps. Both the linear fit over all frequencies and the cubic spline fit underestimated the 4-s ramps. However, some classes of variability seemed to be better suited to each of the four methods presented. For instance, Class 0 and I are best described by either the linear fit over all frequencies or the average PSD from measured data, while Class V data between 30s and 2 minutes is best described by a linear fit over higher frequencies. This suggests that a linear combination of methods, with a different set of coefficients to weight the contribution of each method, for each class of variability, may yield the most accurate results.

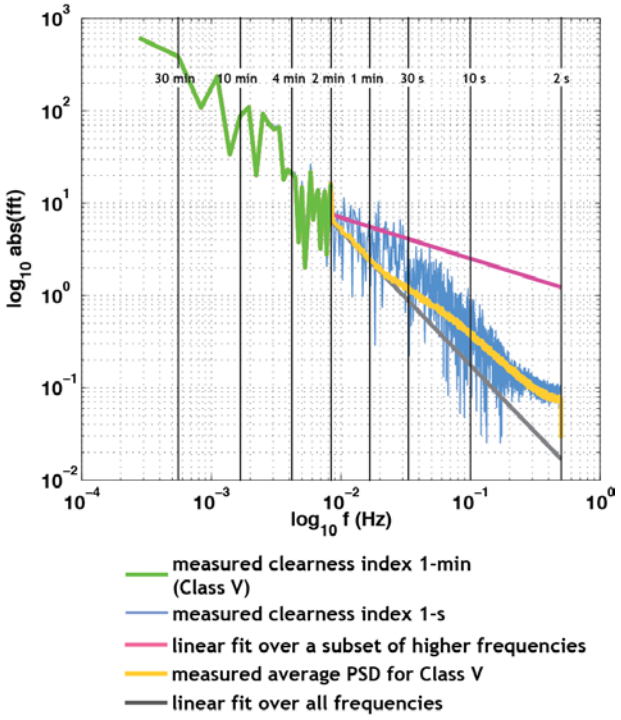

Figure 6. Power spectral density for measured 1-second data, corresponding 1-minute data, and three methods of estimating high-frequency amplitude: linear fit to a subset of frequencies (2-4 minutes), average fit over all Class V data, linear fit to all frequencies in the 1-minute data. Vertical lines are labeled in the corresponding time domain.

V. RESULTS

The weights of the four downscaling methods listed in Table 1 were optimized using a constrained least-squares linear fit. The objective function of the optimization was to minimize the difference between the ramp distributions of the weighted sum of the four methods and the measured data. Table 1 shows the coefficients for calculating a weighted linear sum of the downscaling methods. Spline is the dominant method for the low variability classes (0, I, II, III), which is consistent with our observation that low variability in the 1-minute data is correlated with low variability in the 4-second data. Class V data, which is representative of cumulus cloud movement, is fit primarily by the linear fit to the subset of higher frequencies in the 1-minute PSD. One possible physical explanation for this is that cumulus cloud edges have non-uniform cloud optical depth and move, relative to a point on the surface, on the order of 1 to 20 seconds.

Fig. 8 shows the ramp distributions of measured and modelled 4-second clearness index, for a single site in Colorado. Both datasets have been filtered to represent a 2.4 MW PV plant, covering an area of 0.063 km^2. Each hour of daytime data was classified by the measured 1-minute variability; hours with the same classification were binned together. Table 2 shows both the mean square error for the time series comparison, as well as the 4-s ramp distribution comparison. Clearness index ranges from 0 to 1 for the time series and from 0 to 0.5 for the ramp distribution. Classes 0, I, and II perform extremely well, as expected since the variability of the 1-minute and 4-second GHI is very small. Classes III, IV, and V perform less well in term of mean squared error for the time series. This is also expected given that the modelled data is not meant to predict "when" the 4-second variability occurs in the hour, but is meant to model the frequency and magnitude of the 4-second variability. That is apparent in the low mean squared error of the ramp distributions for all classes.

Table 1. Coefficients for a weighted linear combination of downscaling methods (in time domain), by class of temporal variability.

Downscaling Method	Class of Temporal Variability					
	0	**I**	**II**	**III**	**IV**	**V**
Spline	0.47	0.71	0.44	0.47	0.31	0.32
Linear fit over all frequencies	0.27	0.01	0.28	0.35	0.36	0.22
Linear fit over a subset of higher frequencies	0.11	0	0.11	0.1	0.16	0.45
Spectral amplitude estimated from historical average FFT	0.15	0.15	0.16	0.08	0.17	0.01

Table 2. Mean square error of modelled 4-second clearness index data compared to measured data.

Measure	Class of Temporal Variability					
	0	**I**	**II**	**III**	**IV**	**V**
time series	9.2E-05	6.3E-06	5.2E-04	1.8E-03	1.9E-03	1.6E-02
4-s ramp dist.	6.6E-07	8.8E-11	3.6E-06	9.1E-06	1.0E-05	4.9E-06

CONCLUSION

Solar power studies have moved from questions like "can the grid operate with high penetrations of variable energy?" to "what are the economics to operating the grid with high penetrations of variable energy?" Four-second solar power data enables researchers to investigate new methods of balancing the system under high penetrations of solar power. We present a method of downscaling 1-minute solar data to 4-seconds by optimizing the linear combination of four methods for extending the PSD from f = 1/120 to 1/2 Hz (from 2-minutes to 2-seconds): spline, historic average, full linear fit to PSD, and linear fit to subset of higher frequencies in the PSD. The optimized weights vary by classification of the 1-minute temporal variability. We demonstrate the quality of the fit by observing the mean squared error of the modelled data in both the time series and the distribution of 4-second ramps. The modelled data performs very well in comparing the distributions of ramps, which makes this dataset ideal for use in integration studies concerned with the rapid change in solar power output effecting system balancing requirements.

ACKNOWLEDGMENT

This work was supported by the U. S. Department of Energy under Contract No. DE-AC36-08-GO28308 with the National Renewable Energy Laboratory. The authors gratefully acknowledge the support of Kevin Lynn, Venkat Banunarayanan, and the U.S. Department of Energy Solar Energy Technologies Office SunShot Initiative for funding this work. The authors would like to thank the Measurement and Instrumentation Data Center at NREL for collecting, calibrating, and providing quality control/quality assurance for the measured datasets used in this study.

REFERENCES

[1] Ibanez, E., Brinkman, G. Hummon, M., and Lew, D. (2012) A Solar Reserve Methodology for Renewable Energy Integration Studies Based on Sub-hourly Variability Analysis. *2nd International Workshop on Integration of Solar Power in Power Systems, 12-13 November 2012, Lisbon, Portugal.*

[2] Hummon, M., Ibanez, E., Brinkman, G., and Lew, D. (2012) Sub-Hour Solar Data for Power System Modeling From Static Spatial Variability Analysis. *2nd International*

Workshop on Integration of Solar Power in Power Systems, 12-13 November 2012, Lisbon, Portugal.
[3] Lew, D., Brinkman, G., Ibanez, E., Florita, A., Heaney, M., Hodge, B.-M., Hummon, M., Stark, G., King, J., Lefton, S., Kumar, N., Agan, D., Jordan, G., and Venkataraman, S. (2013). The Western Wind and Solar Integration Study Phase 2. Technical report NREL/TP-5500-55588. National Renewable Energy Laboratory, Golden, CO.
[4] Marcos, J., Marroyo, L., Lorenzo, E., Alvira, D., and Izco, E. (2011) "From irradiance to output power fluctuations - the pv plant as a low pass filter". *Prog. Photovolt: Res. Appl.*
[5] Mills, A. and Wiser, R. (2010). Implications of Wide-Area Geographic Diversity for Short-Term Variability of Solar Power. Technical report LBNL-3884E. Lawerence Berkeley National Laboratory.
[6] Ela, E., Milligan, M., and Kirby, B. (2011). Operating Reserves and Variable Generation. Technical Report. NREL/TP-5500-51978. National Renewable Energy Laboratory.
[7] Ela, E., Milligan, M., and O'Malley, M. (2011). A Flexible Power System Operations Simulation Model for Assessing Wind Integration. Technical report. National Renewable Energy Laboratory.
[8] Weekley, A., Hummon, M., and Searight, K. (2013). Downscaling Solar Power from One Minute to Four Second Time Steps. Technical report. NREL/TP-6A20-60168. National Renewable Energy Laboratory.
[9] Hoff, T. E. and Perez, R. (2013). Evaluating Satellite-Derived and Measured Irradiance Accuracy for PV Resource Management in the California Independent System Operator Control Area. Technical report. Clean Power Research.
[10] Beaucage, P., Brower, M. C., Frank, J. D., and Freedman, J. D. (2012). Development Of A Stochastic-Kinematic Cloud Model To Generate High-Frequency Solar Irradiance And Power Data. Technical report. AWS TruePower.
[11] Sengupta, M. and Andreas, A. (2010). Oahu Solar Measurement Grid (1-Year Archive): 1-Second Solar Irradiance; Oahu, Hawaii (Data). Technical report DA-5500-56506. National Renewable Energy Laboratory.
[12] Kay, S. M. and Marple, S. L. (1981) Spectrum analysis-A modern perspective. *Proceedings of the IEEE,* **69(11)**, 1380-1419.

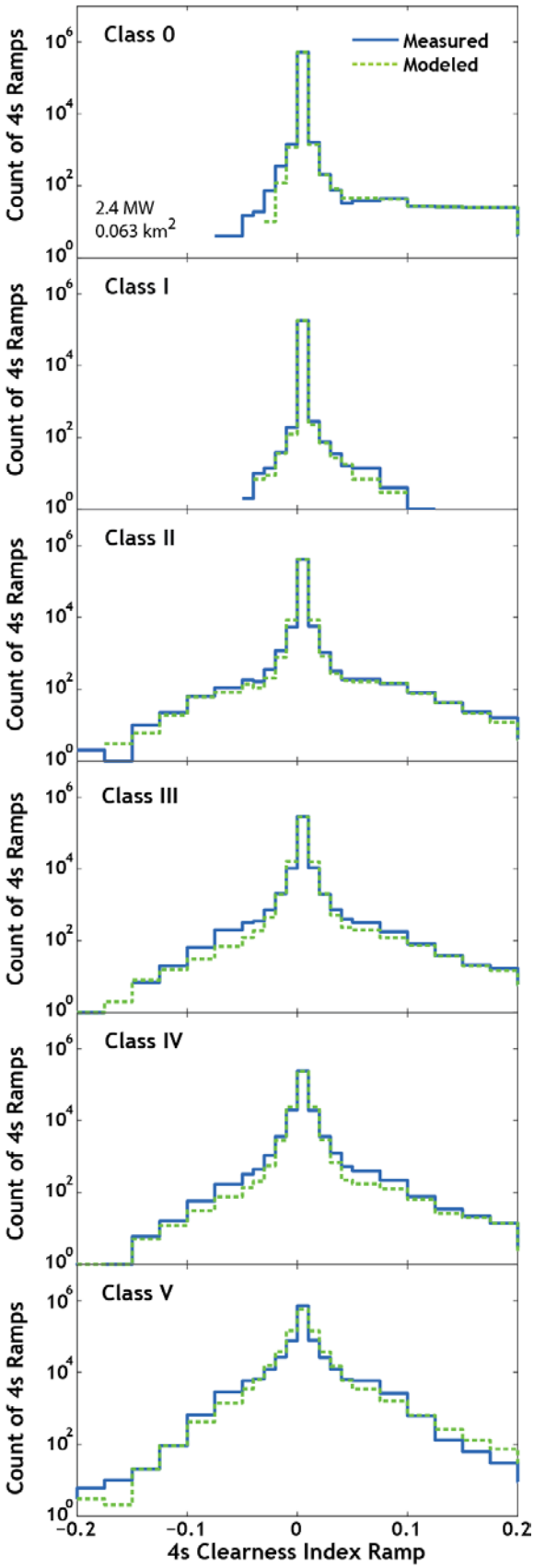

Figure 7. Comparison of 4-s ramp distributions (by variability class) for modelled and measured data.